HUNGARIAN UNIVERSITY OF
AGRICULTURE AND LIFE SCIENCES

Axial flow turbine for solar updraft towers

Thesis of PhD Work

by

Walid Mohammed Abdel-Magid Abdel-Motalb Belal

Gödöllő
2022

Doctoral school denomination: Doctoral School of Mechanical Engineering

Science: Renewable energy

Leader: Prof. Dr. Farkas István, DSc
Faculty of Mechanical Engineering
Hungarian University of Agriculture and Life Sciences, Gödöllő, Hungary

Supervisor: Prof. Dr. István Keppler, PhD
Institute of Technology
Hungarian University of Agriculture and Life Sciences, Gödöllő, Hungary

Dr. Ildikó Molnar, PhD
Faculty of Mechanical and Safety Engineering
Óbuda University, Budapest, Hungary

....

Affirmation of head of school Affirmation of supervisor

CONTENTS

NOMENCLATURE AND ABBREVIATIONS

a, ar	average and local axial induction factors at the rotor
a'	tangential induction factors at the rotor
b	thermal penetration coefficient (W $s^{1/2}$ / m^2 K)
B	number of blades
c	Chord (m)
C_d	drag coefficient
C_l	lift coefficient
C_M	torque coefficient
C_n	normal force coefficient
C_{p3}	pressure coefficient at the diffuser outlet
C_P	power coefficient
C_t	tangential force coefficient
C_T	thrust coefficient
dA	elementary area (m^2)
dM	elementary torque (N m)
dP	elementary power (W)
g	gravitational acceleration (m/s^2)
h	heat transfer convection coefficient (W/m^2 K)
H_c	chimney height (m)
h_r	radiation heat transfer coefficient (W/m^2 K)
H_R	roof height above the ground (m)
k	specific heat ratio
K	thermal conductivity (W/m K)
I	solar irradiation (W/m^2)
$\dot{m}$	mass flow rate (kg/s)
p	pressure (Pa)
P	output power(W)
T	absolute temperature(K)
U_b	ground heat transfer coefficient (W/m^2 K)
U_t	collector loss coefficient (W/m^2 K)
V	air velocity(m/s)
w	total induced velocity (m/s)
W	relative velocity (m/s)
x	local-speed ratio

Greek symbols

α	angle of attack, rad
α_p, α_c	absorptivity of the ground and the cover
β	area ratio
γ	diffuser velocity ratio
ε	velocity ratio
θ	twist angle, rad
λ	tip-speed ratio
ϕ	flow angle, rad
Ω	angular speed of the turbine (rad/s)

1. INTRODUCTION AND OBJECTIVES

In this chapter, the importance of the research topic and brief description of the solar chimney power plant are presented along with the objectives of this research.

1.1. Introduction

Energy drives all modern economic systems. With the rapidly growing world population, more energy should be produced to satisfy rising human requirements and to maintain the welfare. So, harvesting energy on a large scale is undoubtedly one of the main challenges of our time. The global energy demand has continued to increase, but the means of meeting this demand have been mainly the use of non-renewable energy resources. More than 78% of the world's energy consumption in 2013 was supplied directly from fossil fuels, which also provides about 2.6 % from nuclear energy and 19% from renewable energies. With the increasing need for energy and limitation of fossil fuel resources, human beings are more aware of the importance of renewable energies, according to Fig. 1.1 (Arzpeyma et al. 2019). Using non-renewable energy supply sources such as fossil fuel burdens the environment with greenhouse gas emission and global warming, while the flared hot flue gas causes global warming in the atmosphere where the process occurs. The power generation sector was the highest contributor to global greenhouse gas emission in 2005 which accounted for about 25 percent of global greenhouse gas emission (Al-Kayiem and Aja, 2016).

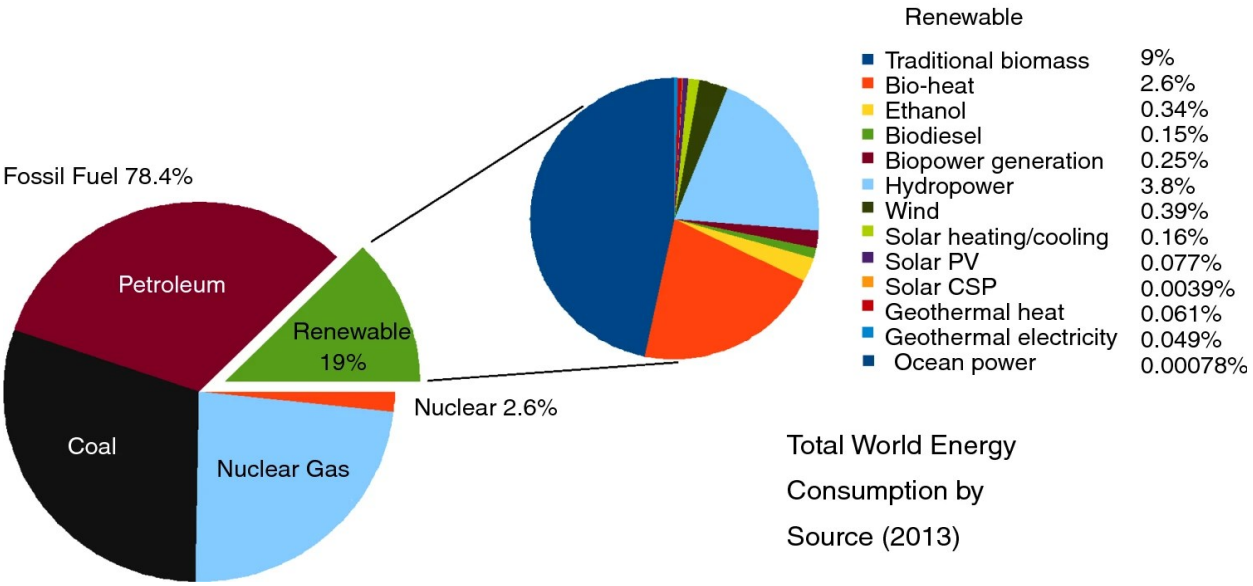

Fig. 1.1. Statistical analysis of world energy consumption (Arzpeyma et al., 2019)

Solar energy is the most abundant and well distributed form of renewable energy. Many solar technologies are used to harvest the sun's energy throughout the world. The annual renewable energy supply exceeds the global energy demand shown in the previous section on evolution of the world energy demand by several orders of magnitude. 6.48×10^{18} MJ of solar energy reaches the surface of the Earth, which is about ten thousand times more than the annual global primary energy demand and much more than all available energy reserves on our planet (Quaschning, 2014). This solar energy reaches earth in two forms: direct and indirect solar energy. Solar technical systems using direct solar energy convert incoming solar radiation directly into useful energy, for instance, electricity or heat. Wind, river water and plant growth are indirect forms of solar energy. However, natural processes convert solar energy into other types of energy, then, other technical systems can use these indirect types of solar energy as well.

The most promising solution is an extension of using the renewable energy source, consequently, renewable energy gradually can be the main source of the world energy system (Guo et al., 2019). Solar chimney power plant (SCPP) is a new technology that utilizes renewable energy sources to produce electricity, for achieving its goals, it uses the combination of solar heating and chimney effect. The SCPP has low-efficiency but is favoured with well-developed technologies that make up the system. The materials for the development of the system are easily sourced locally. Thus, the plant has a promising future as a large-scale solar-electric power plant. The SCPP is characterized by a long lifespan, little maintenance, no combustible fuel, no cooling water and it is free of greenhouse gas emissions. The SCPP technologies are simple, reliable and can be developed in technologically less developed countries, which are sunny and often have limited draw material resources for other advanced technologies.

1.2. The main research objectives

The objective of this research is to design axial single stage turbine to obtain the maximum output power possible from SCPP. The design of an axial flow turbine is presented based the Blade Element Theory (BET), which is modified to improve the performance of the wind turbine by the concept of Argument diffuse wind turbine (ADWT). I also used the mathematical model to predict the expected output power. According to the characteristics of the solar chimney turbine, blade element theory is chosen to design solar chimney turbine. An aerodynamic analysis accounting the surrounding diffuser duct is presented, which defines parameters of the design.

My comprehensive mathematical model is used to calculate the design parameters. My The mathematical model depends on easily measurable quantities to estimate the performance of SCPP. The performance of the whole SCPP system is accurately analysed by using CFD simulation model, with fewer assumptions in the theoretical calculation, but more detailed description of pressure and flow field could be obtained. A 3D approach for SCPP prototype is carried out by using ANSYS CFX v18 with axial vertical flow turbine. I manufactured the solar chimney turbine by using the 3D printing technology. The blade calculations were according my new approach of BET, which consider the surrounding duct. I have tested my newly designed turbine blades using a wind tunnel of 1m diameter and 8 m length. I measured the electrical output power, pressure difference around the turbine and airflow rate to calculate dimensionless parameters. Therefore, the following methods could be used in the research to accomplish the following objectives and tasks:

- Investigation of the performance of the SCPP by mathematical model to deeply understand the concept of SCPP and calculate the parameters of the turbine design.
- Estimation of the performance of the SCPP with different collector shapes by CFD simulation.
- Comparison of the different theories of the turbine design using evaluation of their performance within the SCPP simulation.
- Solution of the blade element theory (BET) equations with the diffuser duct effect to make the blade more sensitive and to have efficient performance.
- Testing the performance of the turbine using wind tunnel measurements.

2.MATERIALS AND METHODS

Using sustainable energy has many scientific and technical challenges due to non- concentrated resources, which reduces the efficiency of devices that used to harvest renewable energy. Solar chimney power plant (SCPP) is a new technology that depends on renewable energy sources. To raise its reliability and expansibility, efficient design of the solar chimney system components is an utmost necessity. A turbine is a key component because it captures the mechanical energy from airflow. The conditions of operation of the turbine inside SCPP impose particular characteristics of the turbine, these characteristics for the turbine are between a gas turbine and wind turbine. The efficient design of the turbine achieves the maximum output power from the SCPP unit.

In this chapter, I proposed the materials and methods of the new solar chimney turbine design, my comprehensive mathematical model is also presented to determine the new design parameters, that calculate the flow field conditions on the critical point on SCPP system. The performance of SCPP is investigated by CFD model and experiments.

2.1. Aerodynamic analysis of a shrouded turbine

The aerodynamic analysis of the wind turbine consists of the actuator disc theory that applies the momentum concept on the infinite number of the blade rotor, the rotor disc theory that takes into account the rotation effect of the rotor, and the blade element theory (BET) that considered the force acting on an element of the blade. The analysis is incorporated with the diffuser duct effect to make the blade more sensitive and to have efficient performance during its working inside the duct. By solving equations of the BET theory, the chord distribution and twist angle are obtained presenting the final shape of the blade turbine.

2.1.1.Rotor disc theory considering surrounding duct

The actuator disk theory does not consider the wake rotation, but the rotation of the wake is an essential effect to produce the power. It defines the tangential induction factor, *a*', that has an enormous influence on the shape of the blade turbine and subsequently its performance. By undergoing an infinitesimal control volume of an area $dA = 2\pi r dr$, to apply the angular momentum equation the elementary available torque *dM* can be obtained as:

$$dM = \rho V_1 w r^2 dA = 2\rho a' \gamma (1-a) V_0 \Omega r^2 dA \tag{2.1}$$

where *r* is the radial position on the blade from hub to tip, *w* is the angular velocity of air in the near- wake, $w = 2\Omega a'$, and Ω is the rotor angular velocity (Burton *et al.*, 2011).

The torque coefficient is defined as:

$$C_M = \frac{dM}{\frac{1}{2}\rho V_0^2\, dA} = \frac{4a'\gamma(1-a)\Omega r^2}{V_0}\,. \tag{2.2}$$

The elementary produced power is calculated by:

$$dP = \Omega dM = 2\rho a' \gamma (1-a) V_0 \Omega^2 r^2 dA\,. \tag{2.3}$$

By integrating this expression across the rotor from *r = 0* to *r = R*, the power coefficient is obtained by:

$$C_P = \frac{P}{\frac{1}{2}\rho A V_0^3} = \frac{8}{\lambda^2}\int_0^{\lambda} \gamma a'(1-a) x^3 dx, \tag{2.4}$$

where λ is the tip-speed ratio, $\lambda = \Omega R/V_0$, and x is the local-speed ratio, $x = \Omega r/V_0$.

2.1.2. Blade element theory considering surrounding duct

After studying the effect of the diffuser on the turbine performance using the actuator disc theory and rotation effect, forces acting on the blade are obtained by applying the blade element theory (BET). The BET suggests that the blade is to be divided into N sections, there is no aerodynamic interaction between blade sections. The blade sections are called blade elements. The forces acting on the blade elements are determined solely by the drag and lift coefficient of 2D aerofoils of the blades. Consequently, the aerodynamic forces which have an effect on the turbine blades are also expressed as a function of lift and drag characteristics of the aerofoil and the aerofoil's characteristics depend on the angle of attack and Reynolds number. Fig. 2.1 shows the velocity diagram and forces acting on the section of the rotor blade element.

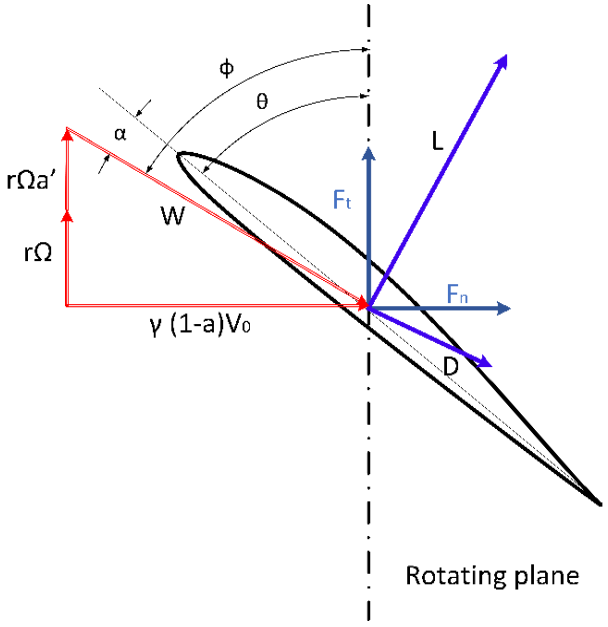

Fig. 2.1. Blade Element forces and velocity diagram

The flow angle can be obtained by the velocity diagram shown in Fig. 2.1:

$$\tan \emptyset = \gamma \frac{(1-a)V_0}{(1+a')\Omega r} = \gamma \frac{(1-a)}{(1+a')x}. \tag{2.5}$$

From Fig. 2.1, the elemental normal and tangential force coefficients at any section of a blade are defined as:

$$C_n = \frac{F_n}{\frac{1}{2}\rho W^2 c} = C_l \cos \emptyset + C_d \sin \emptyset \tag{2.6}$$

and

$$C_t = \frac{F_t}{\frac{1}{2}\rho W^2 c} = C_l \sin \emptyset - C_d \cos \emptyset \tag{2.7}$$

respectively. Where C_l and C_d are the lift and drag coefficients of the airfoil respectively.

The axial induction factor can be obtained:

$$\frac{a}{1-a} = \gamma^2 \frac{BcC_n}{8\pi r \sin^2 \emptyset} \ . \tag{2.8}$$

The tangential induction factor can be obtained:

$$\frac{a'}{1+a'} = \frac{BcC_t}{8\pi r \, sin \emptyset \cos \emptyset}. \tag{2.9}$$

The actuator disc theory assumes an infinite number of blades for a turbine rotor, however, Prandtl introduced the concept of a tip loss to account for the difference between a real turbine or propeller that having a finite number of blades and theoretical one (Clifton-Smith, 2009). To determine the optimum blade shape for maximum produced power, the refinement of BET by tip loss corrections is important. The tip loss factor, *F*, is defined as the ratio of the azimuthally averaged axial induction factor, *a*, to the axial induction factor local to the blade, a_r.

The induced velocities and the mass flux influence by the tip loss correction, sequentially, Eqs. 2.8 and 2.9 is corrected according to Shen *et al.*,(2005):

$$\frac{a_r F(1-a_r F)}{(1-a_r)^2} = \gamma^2 \frac{BcC_n}{8\pi r \sin^2 \emptyset} , \tag{2.10}$$

$$\frac{a' F(1-a_r F)}{(1+a'_r)(1-a_r)} = \frac{BcC_t}{8\pi r \, sin \emptyset \cos \emptyset}. \tag{2.11}$$

Vaz and Wood, (2016) expressed the tip loss factor that take into consideration the diffuser duct by term the diffuser velocity speed-up ratio,γ , as :

$$F = \frac{2}{\pi} \cos^{-1} e^{-f} , \tag{2.12}$$

where $f = \frac{B}{2} \frac{W(R-r)}{r\gamma(1-a_r)V_0}$

the above discussion clearly shows the effect of the diffuser duct on the blade element theory by the diffuser velocity speed-up ratio term. The main challenge is a way to obtain this value, γ. Vaz and Wood, (2016) used the average of the experimental data, which was carried out by ten Hoopen, (2009) to obtain the value of the diffuser velocity speed-up ratio.

2.2. Mathematical model of Solar Chimney

Solar chimney power plants (SCPPs) convert solar energy first into thermal energy then into kinetic energy and finally into electrical power. According to the operational principle mentioned in the introduction section, a mathematical model is presented here to study physical phenomena for main SCPP plant components (collector, chimney and turbine). The aim of this model is to calculate the essentials terms of the turbine design.

The mathematical model studies the performance of the SCPPs by obtaining the properties of the flowing air at the critical points, which are indicated in Fig. 2.2. Point ① has known value, it is the ambient condition. I presented a new approach of heat transfer patten inside the collector to develop the mathematical model that can elevate the performance of SCPP with more accuracy. In the next sections, the properties of air in other points will be determined.

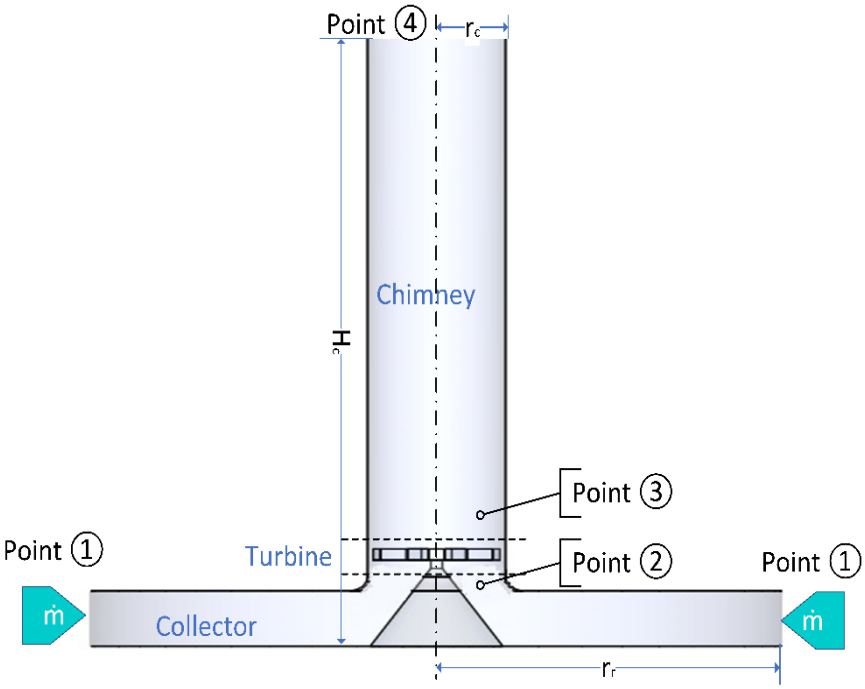

Fig. 2.2. Schematic mathematical layout of solar chimney power plant

2.2.1. Collector

I have been studied thermal analysis for the solar collector in considerable detail to understand the performance of the SCPP and I have been developed the thermal network to demonstrate the different heat transfer patterns inside the solar collector of SCPP. Fig. 2.3.a shows the different surface of the collector and heat coefficients undergo it, and Fig. 2.3.b shows the equivalent thermal network.

By applying the heat balance on the critical point as:

at point T_c: $S_1 + h_1(T_f - T_c) + h_{r,p-c}(T_p - T_c) = h_w(T_c - T_1) + h_{r,c-s}(T_c - T_s)$ (2.13)

at point T_f: $h_1\,(T_c - T_f) = q_f + h_2\,(T_f - T_p)$ (2.14)

at point T_p: $S_2 = h_2(T_p - T_f) + h_{r,p-c}(T_p - T_c) + U_b(T_p - T_G)$ (2.15)

Where, $S_1$and S_2 are the solar radiation which reach to collector cover and surface of the ground respectively. h_w is the convection heat transfer between the surrounding and the outer surface of the cover. $h_{r,c\text{-}a}$ is the radiation heat transfer coefficient between the outer surface of the cover and surrounding . h_1 and h_2 are the convection heat transfer coefficient between the inner surface of the cover and the air, and the surface of the ground and the air respectively. q_f is the gain useful heat in the air. $h_{r,p\text{-}c}$ is the radiation heat transfer coefficient between the surface of the ground and the inner surface of the cover. U_b is the ground heat transfer coefficient.

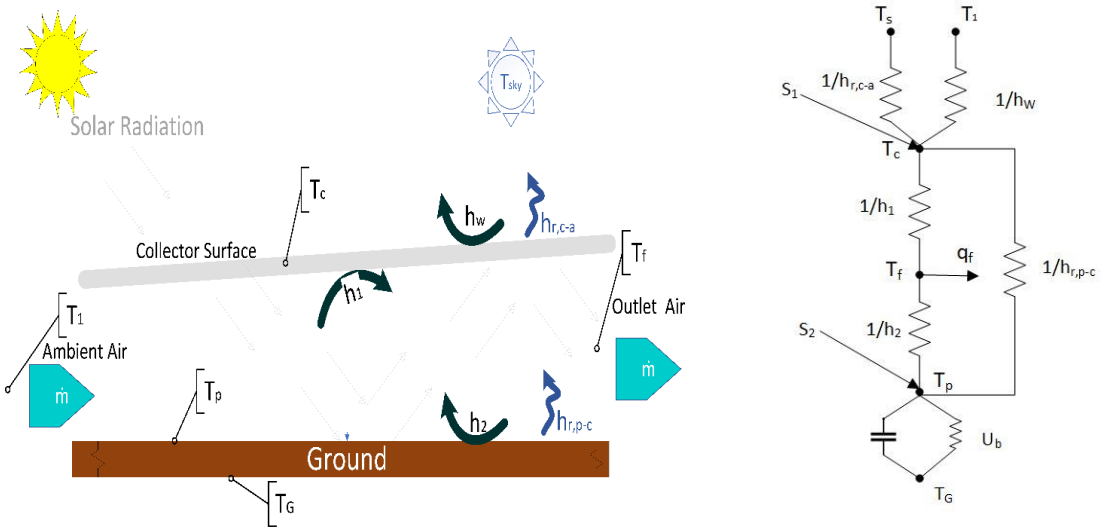

a. Heat transfer coefficient and surfaces b. Thermal network

Fig. 2.3. Thermal model for the collector

The temperature of the air changes with the radial position of the collector. Thus, Eqn. 2.13-2.15 should be solved in different radial positions to find the temperature distribution inside the collector.

The useful heat can be expressed as a function of the air temperature as:

$$q_{r,i} = \frac{\dot{m}c_p}{A_i}\left(T_f - T_{f,i}\right) = \mu_i\left(T_f - T_{f,i}\right) \tag{2.16}$$

Where $\dot{m}$ is the mass flow rate through the SCPP, and A_i is the area of the collector at the radial position. i is a radial position of the collector in the range r_r to r_c.

By substituting Eqn 2.16 into Eqn 2.16 and rearranging, a 3x3 is matrix obtained:

$$\begin{bmatrix} \left(h_1 + h_{r,p-c} + h_w + h_{r,c-s}\right) & -h_1 & -h_{r,c-s} \\ +h_1 & -(h_1 + h_2 + \mu_i) & +h_2 \\ -h_{r,p-c} & -h_2 & (h_2 + h_{r,p-c} + U_b) \end{bmatrix} \begin{bmatrix} T_c \\ T_f \\ T_p \end{bmatrix} = \begin{bmatrix} S_1 + h_w T_a + h_{r,c-s} T_s \\ \mu_i T_{f,i} \\ S_2 + U_b T_G \end{bmatrix}.$$

For simplicity, the above matrix can be expressed as:$[H][T] = [S]$, the mean temperature vector can be calculated using matrix inverse technique as:

$$[T] = [H]^{-1}[S]. \tag{2.17}$$

The calculation of the temperature vector [T], is accomplished by assuming an initial value of temperatures, because the matrix coefficient [H], depended on the resultant temperatures vector [T], while computing the final value by employing iterative techniques, now, the temperature of the point ② is determined, which equal the temperature at, r_c, the smallest radial position, T_f. To calculate the condition of point ②, the equations for continuity, momentum and energy of the flow under the roof were applied by Koonsrisuk and Chitsomboon, (2013), which is expressed as:

$$p_2 = p_1 + \frac{\dot{m}\, q_r}{2\pi H_R^2 \rho_1 c_p T_1} \ln\frac{r_r}{r_c} - \frac{\dot{m}^2}{2\rho_1}\left(\frac{1}{A_2^2} - \frac{1}{A_1^2}\right). \quad (2.18)$$

To describe the performance of a solar collector, an energy balance analysis indicates the distribution of incident solar energy into useful energy gain, thermal losses, and optical losses. In steady state analysis, the solar radiation absorbed by a collector per unit area of absorber *I* is equal to the difference between the incident solar radiation and the optical losses, which can be expressed as:

$$q_r = I(\alpha_c) - U_t\ \Delta T \quad (2.19)$$

Where α_c is absorptivity of glass cover, U_t is collector loss coefficient (W/m^2 K), ΔT is the temperature difference between the air inside and outside a solar collector.

2.2.2.Turbine

A turbine of the solar chimney has an enormous influence in the SCPP plant as that extracts the kinetic energy from the hot air and transmits it to the generator. The conventional layout of the solar chimney turbine is of the axial flow type. The specifications for large wind turbines are in many aspects similar to those ones of solar chimney turbines (Tingzhen *et al.*, 2008a) (Zhou *et al.*, 2016). The solar chimney turbine and traditional wind turbines both convert large amounts of kinetic energy in the airflow at low temperature to mechanical energy.

From the energy equation and Gibbs relation from classical thermodynamics, the theoretical power extracted by the turbine can be calculated as:

$$P = \dot{m}\int v dp = \frac{\dot{m}}{\rho_{tur}}\ \Delta p_{tur}\ = 2\,\dot{m}\,\frac{(p_2 - p_3)}{(\rho_2 - \rho_3)}\,. \quad (2.20)$$

The streamline of the flow subject to change in direction by 90° at the entrance to the chimney, thus, the flow area becomes less than the chimney area which is known as vena contracta phenomena. Consequently, the highest velocity in the chimney is located near the entrance of the chimney where we have the location of the smallest flow area. This phenomenon is shown clearly in the result of computational fluid dynamics (CFD) by A.Elmagid and Keppler, (2017). The contraction coefficient, *CC*, is a ratio between the vena contracta area and the entrance (original) area. Batchelor, (2000) applied the streamline theory for two dimensional cases by supposing that the orifice is simply a hole in a plane wall of small thickness, then, the conclusion that the contraction coefficient is 0.61, which agrees with the experimental data. The contraction occurs within a distance from the aperture of 0.4 of its diameters.

To obtain the diffuser velocity speed-up ratio, the continuity equation is applied between point ② and ③ in Fig. 2.2 :

$$\dot{m} = A_2 V_0 \rho_2 = 0.61 A_2 V_t \rho_3 \quad (2.21)$$

Then

$$\gamma = \frac{V_t}{V_0} = \frac{\rho_2}{0.61\rho_3} \quad (2.22)$$

Eq. 2.22 calculates the diffuser velocity speed-up ratio, which is the parameter making the blade to be sensitive to surrounding duct. So, a more suitable blade for SCPP environment can be

designed by above design procedure. The mathematical model and aerodynamic design are a function of the mass flow rate that is taken from experimental data.

2.3. Optimal design of blade geometry

The main purpose of most turbines is to extract as much energy from the flow of the fluid as possible, and the different components of the turbine has to be optimized for achieving that goal. Thus, optimizing a blade design is a substantial aim of this study using a suitable solution to blade element-momentum equations, Eq. 2.3, which is incorporated with the diffuser duct. Additionally, making this design efficiently works inside SC by defining design terms of SC parameters.

The maximization of the power coefficient is done by maximizing the integrand of $a'(1-a)$ in Eq. 2.4 as:

$$\frac{d}{da}[a'(1-a)] = (1-a)\frac{da'}{da} - a' = 0 \tag{2.25}$$

Eq. 3.48 is valid only if the aerofoil works under the stall region. Consequently, the relative velocity and acting force on the aerofoil are acting in the same direction as shown in Fig. 2.1, according to notes by Wood, (2015). He also showed that λ should be around 1 or greater (λ > 1). Under this condition, (Vaz and Wood, 2016) expressed:

$$x^2 a'(1+a') = \gamma^2 a(1-a). \tag{2.26}$$

Using the differential Eqs. 3.12 and 3.48:

$$(1+2a')\frac{da'}{da}\left(\frac{x}{\gamma}\right)^2 = 1-2a. \tag{2.27}$$

The optimum relation between *a* and *a'* is given by combining Eqs. 3.48, 3.49, and 3.50 as:

$$a' = \frac{(1-3a)}{(4a-1)}\ , \tag{2.28}$$

the same relation for a bare turbine is derived by Glauert, (Vaz and Wood, 2016).

To find the optimum relation between *x* and *a*, Eqs. 2.26 and 2.28 are substituted to obtain:

$$16\,a^3 - 24\,a^2 + \left[9 - 3\left(\frac{x}{\gamma}\right)^2\right]a + \left[\left(\frac{x}{\gamma}\right)^2 - 1\right] = 0. \tag{2.29}$$

The optimal design of the blade is implemented by solving the blade element theory at a different radial position using MATLAB. Vaz and Wood, (2016) used the initial guess and damping error technique to solve Eq. 2.27, but in I have been used the *root* command in MATLAB my model to find exact solution of Eq.2.29. To obtain the correct root of the equation, the range from 0.2 to 0.5 is set according to results of Wood, (2015). The optimization procedure of the blade can be considered as a function of the induction factor*, a*, once the blade element lift and drag are available. So*, Xfoil.m* is a MATLAB function that works as a system called to run *XFoil* program. It then loads the results data of the aerofoil into a structure which you can then use in iterative algorithm.

2.4. CFD model of solar chimney

Nowadays, using computational fluid dynamic (CFD) is possible to model the whole solar chimney system. However, principles of solar chimney power plants depend on many physical

phenomena such as heat storage, turbomachinery, and radiation heat transfer, which increase the level of the complexity of analysing the system. To solve the governing equations of a solar chimney system, we used ANSYS CFX v18.1, which solves the conservation equation of energy, momentum, and mass with K-omega turbulence model.

To calculate radiation heat transfer, we use two radiation model: P-1 model solve the fluid domain and Monte Carlo model solve the solid domain as Surface-To-Surface configuration. The interface between turbine domain that has the rotational motion with collector and chimney domains involve the sliding mesh. We should apply frozen rotor model to solve this sliding mesh.

The buoyancy phenomena have an enormous effect in the solar chimney system, so, the buoyancy model is used. Buoyancy effects can be simulated using one of two available models in ANSYS CFX; Full Buoyancy Model (Density Difference) and Boussinesq Model, it switches between them according to the properties of a fluid.

Full Buoyancy Model (Density Difference): For single-phase flows, this model is used when the fluid density is a function of temperature or pressure (which includes all ideal gases and real fluids). Significant density variations with temperature occur for most gases. You should specify a Buoyancy Reference Density as an approximate average value of the expected domain density.

Boussinesq Model: For many applications involving buoyancy, it is sufficient to assume a constant fluid density when the change in density over the expected range of conditions is relatively small. This is often true for many liquids. When the fluid density is not a function of pressure or temperature, the Boussinesq model is employed. The Boussinesq model uses a constant density fluid model, but applies a local gravitational body force throughout the fluid that is a linear function of fluid thermal expansivity, and the local temperature difference with reference to a datum called the Buoyancy Reference Temperature. You should specify the reference temperature as an approximate average value of the expected domain temperature (ANSYS CFX-Solver theory guide).

As mentioned, the SCPP unit consists of ground, cover collector, chimney and fluid zone. All component geometry is drawn as 3D using SOLIDWROKS, as shown in Fig. 2.4 (light green is Cover collector, blue is Fluid zone and yellow is ground area). The ANSYS Design Modeler is used to enter CAD file, which is a part of ANSYS Workbench 18. It able to read CAD file and transfer data reading to grid generation program such as Meshing or turbo grid. However, ANSYS Meshing is used that suitable for SCPP geometry. This technique has many advantages, reading shape with high accuracy and save time and labour needing to enter data. The geometry of SCPP in Fig. 2.4 is divided into three zones: the first zone is the fluid section that has a blue colour, the second zone is the ground section that has a brown colour and the third zone is the glass cover of the collector that has a green colour. This division process gives us the ability to use different materials domain on the ANSYS CFX model.

Grid generation is very important to generate accurate grids for the solver to obtain correct results. The accuracy of the CFD solution depends on the quality of the grid used to perform the calculations. The accuracy of the CFD calculations depends on the quality of the grid that is used.

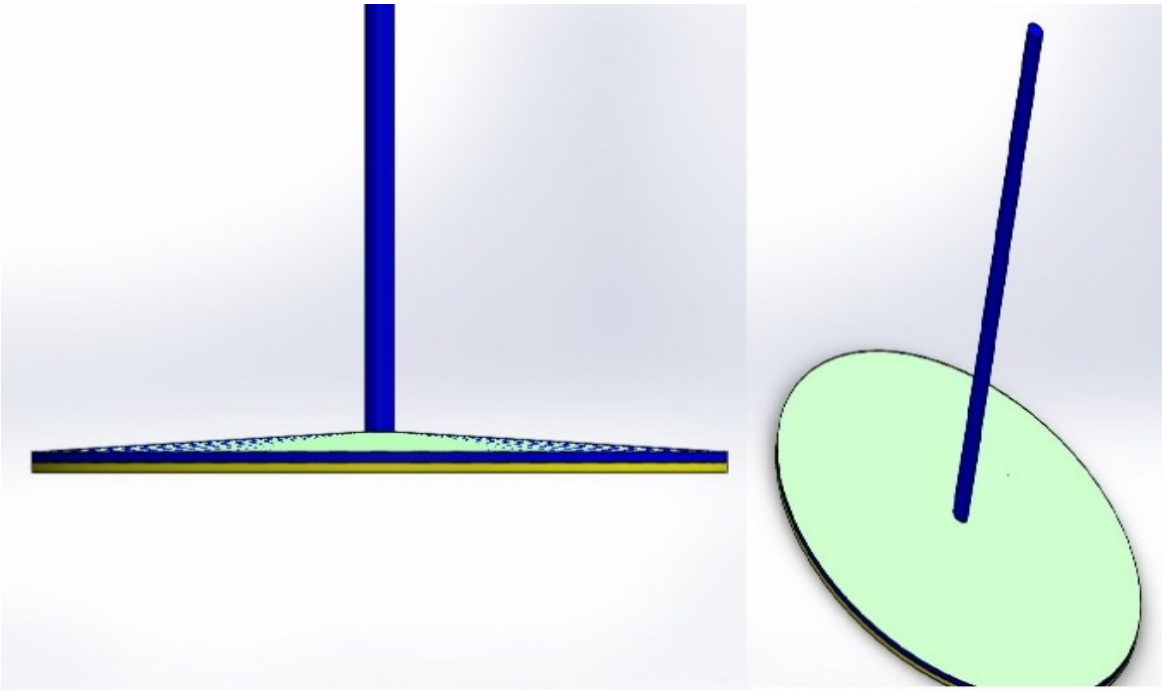

Fig. 2.4. Three-dimension geometry of solar chimney prototype

The calculation of the model with different number of nodes has been carried out as show in Fig. 2.5 The theoretical outpower and mass flow rate through the turbine is chosen to compare the output results and decide the appropriated number of nodes, the calculation show that the around 2.5 million of the nodes is qualified for this simulation and we used 3 million number of nodes in this model calculation. Table 2.1 shows inlet parameters for model to make grid independence test and the full detail of the boundary conditions are demonstrated.

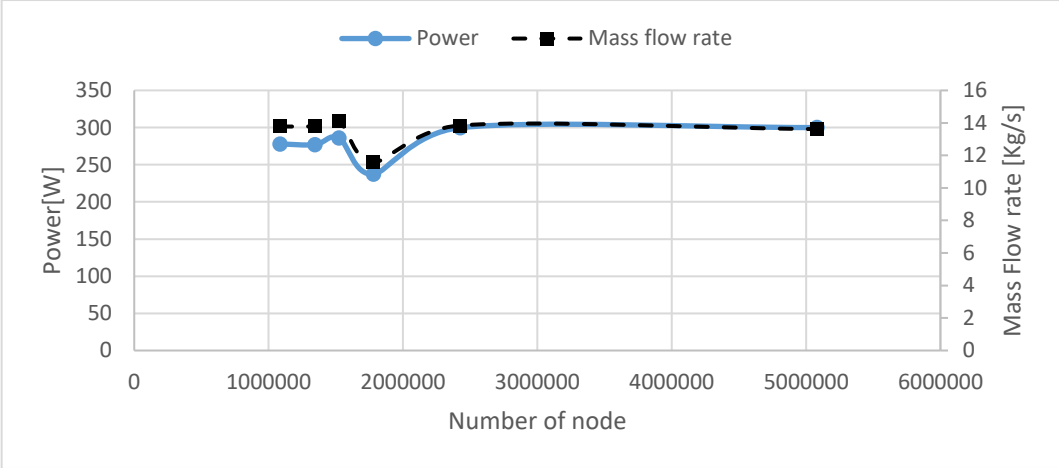

Fig. 2.5. Grid- independence test calculations

Table 2.1 Inlet parameters for grid-independence test

Inlet velocity	8 m/s
Number of turbine blades	4
Rotational speed of the turbine	840 rpm
Diameter of the turbine	1m
Height of chimney	30 m

Boundary conditions have serious implications on the CFD solution. This further reinforces the requirement to define suitable boundary conditions that appropriately mimic the real physical representation of the fluid flow. In many real applications, there is always great difficulty in defining in detail some of the boundary conditions at the inlet and outlet of a flow domain that is required for an accurate solution. A typical example is the specification of turbulence properties (turbulence intensity and length scale) at the inlet flow boundary, as these are arbitrary in many CFD problems. Nevertheless, by carrying out an uncertainty analysis, the reader can develop a good feel of the appropriateness and inappropriateness of the boundary conditions that are being imposed within the physical context of the CFD problem being solved.

The accuracy of the simulation model results substantially depends on the imputed boundary condition. The height of the chimney is considered by evaluating the change of atmospheric pressure with height as well-known that the flow inside the chimney follows up a dry adiabatic lapse rate. Direct radiation and rotational of the turbine are taken from experimental data, because of continuously changing with time. The surface of the ground that contact with air exposed to solar radiation less than outer cover surface by glass transmissivity. To clarify the different performance of collectors within various shapes, Experimental apparatus

The experimental work aims to demonstrate that the designed turbine can operate efficiently over the required range of mass flows and pressure drops that saved by Solar chimney power plants (SCPPs). Additionally, the experiment assists to quantify the turbine performance and gain a better understanding of the turbine operation.

2.4.1. Layout of experimental rig

The rig of the experiment should allow for a detailed investigation of the turbine performance and satisfy the design objectives listed above. In this study, we chose the wind tunnel technique to test the solar chimney turbine, a wind tunnel is usually used for testing turbomachines because it saves the criteria of the operation condition during testing by strictly controlling inflow conditions. The blades and hub are a main construction of the conventional axial flow turbine; the blade consists of the aerofoils that interact with the hot air and convert the power in the air to mechanical power. The geometry and dimensions of the blades are determined by characteristics flow of SCPP to make it an optimum. 3D printing is used to manufacture blades of turbine prototype according to calculations that is shown in detail in above.

The tested prototype comprises the four-blade turbine rotor, which connects to the electrical generator that working as the load of the turbine. The hub is the part that transmits all the power and loads from the blades to the generator shaft. We designed the hub as two prats that makes it can change the angle of the blades, and easy to manufacture and assemble by 8 bolts. Fig. 2.6 shows the prototype hub, which manufactured of polyethylene.

The electric system takes a part of our measurement, comprises the generator and electric heater, works as a load of the turbine. A 1800A007 Mitsubishi Alternator was used on the measurement, it is designed for the car Diesel engine, therefore; the challenge comes. The range of the rotational speed of the car engine is higher than the turbine ones. I get a lot of help from Mr. Gábor Bércesi, a Ph.D. student to modified the exiting circuit of the generator. This change makes the generator is more suitable for a rotational speed range of the turbine.

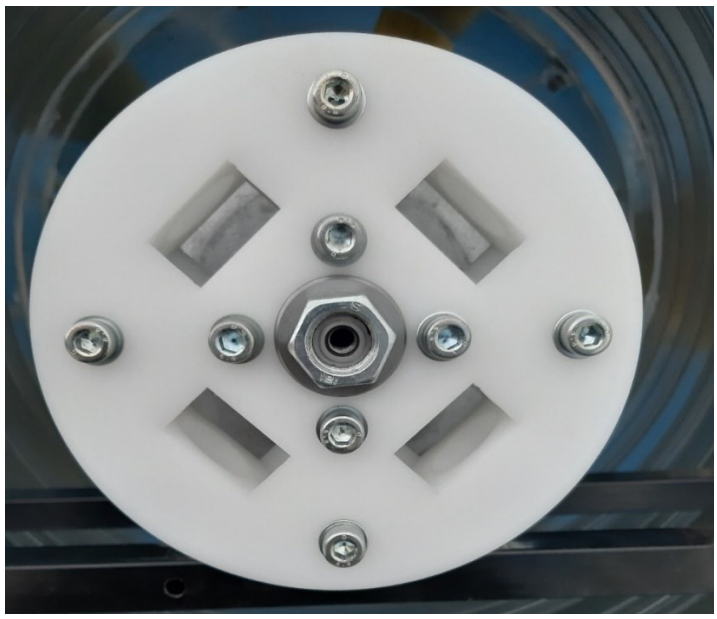

Fig. 2.6. The hub of the tested turbine

The experiment is carried out in the energy laboratory, Szent István University at Gödöllő campus. We used the wind tunnel, 8 m of length and 1 m of the square/circle cross-section, as shown in Fig. 2.7. Its first block from the inlet side has the laminar basket for damping the inference of surrounding. The draft fan connects with the suitable inverter, the inverter saves a proper control of the rotational speed of the fan, consequence, providing the control of the airflow velocity.

Fig. 2.7 The wind tunnel at Szent István University at Gödöllő campus

2.4.2. Measurement strategy

To evaluate the performance of the solar chimney turbine from the experimental rig, certain physical properties have to be measured, then, the dimensionless variables have to be determined from this measured quantity. The Physics quantity as:

- Airflow velocity, v_{in}
- Pressure drops around turbine, $\Delta p_{tur,st}$
- DC Voltage, V
- DC Current, I
- Outside Air temperature and humidity
- Reference pressure
- Rotational speed of the turbine

Fig. 2.8 shows the schematic and layout of the wind tunnel testing for the designed turbine. After fixation the rotor of the turbine on the generator shaft and the prob of the sensors as shown in Fig. 2.8, the procedure of the solar chimney turbine will be carried out by following the next steps:

1- Turn on the fan on the low speed and check the sensors reading on the laptop screen.
2- Adjust the fan on the required speed by setting frequency as 10, 15, 20,25 then 30 Hz and waiting for few minutes to achieve steady state operation.
3- Change excitation voltage of the generator
4- Start recording the data logger and manual reading (Cooling water temperature, electric power, voltage, and current) for about 15 minutes
5- Stop the fan and prepare to the next reading
6- Repeat the above steps with a new speed

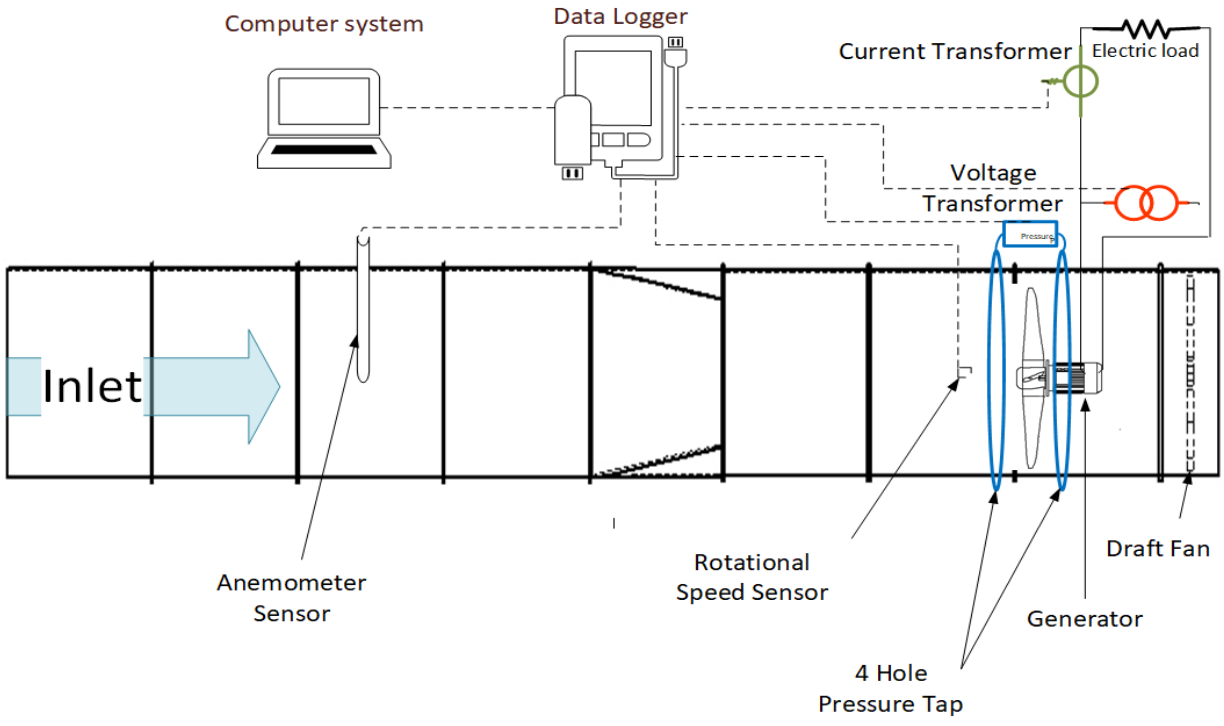

Fig. 2.8. Schematic diagram of testing the turbine within wind tunnel

3.RESULTS AND DISCUSSIONS

In this chapter, the theoretical results of both mathematical and CFD models of a solar chimney power plant (SCPP)are presented and discussed. We explain how to use the presented result in aerodynamic theories to get the turbine. The main finding of this study is a new design of the solar chimney turbine that is also presented in this chapter. Finally, the results is shown the performance of SCPP with new turbine.

3.1. The mathematical model of solar chimney power plant

As showing the comprehensive mathematical model that I improve on many points, it depended on easily measured parameters such as ambient conditions and up-wind velocity of the chimney, additionally optical material properties. Table 3.1 shows Manzanares SCPP prototype dimensions that are adopted from results of Haaf, (1984) and constant values that are used on the calculations. The measured data was carried out at noon (12:00) of September 2nd, 1982. The optical properties of the SCPP material was found in detail in (Haaf *et al.*, 1983) and (dos S. Bernardes, Voß and Weinrebe, 2003). To validate the mathematical model, calculated results are compared with the experimental results of the prototype from Manzanares, Spain, as shown in Table 3.2 accorded at 12:00. The deviation of the collector loss coefficient, the collector exit temperature, the pressure drops of the turbine, and output power are 1.808%, 5.943%, 6.668% and 0.5909% respectively, which are acceptable value.

Table 3.1. Geometrical dimensions and constant value of the pilot plant in Manzanares, Spain

Geometrical dimensions	
Mean roof radius, r_r	122 m
Average roof height, h_R	1.85 m
Tower height, h_c	194.6 m
Tower radius, r_c	5.08 m
Physical constant value	
Thermal conductivity, k	0.0321 W/m K
kinematic viscosity, kv	24.11e-6 m^2/s
Collector absorption coefficient, α	0.6897
Cover emittance (Glass optical properties), ε	0.9
Stefan-Boltzmann constant, σ	5.6697e-8 $W/m^2 K^4$
Constant Pressure Heat coefficient, cp	1000.5 J/Kg.k

Table 3.2. Comparison between measured data and theoretical results

	Measured	Calculated	Error
Collector loss coefficient, U_t (W/m² K)	15	14.7288	1.808%
Temperature at collector exit, T_2 (°C)	38	40.2583	5.943%
Pressure difference of turbine, Δp_{tur} (mbar)	0.75	0.7	6.668%
Power, P (kW)	48.4	48.686	0.591%

Using Eq. 2.22, the main aim of the mathematical model is achieved by obtaining the value of the diffuser velocity speed-up ratio be 1.6403 at the design point that is shown by Haaf *et al.*, (1983). Fortunately, this value is near the value shown by Phillips, (2003). Also, he found that the diffuser efficiency of 0.8, the optimal value are an $a_{opt}=0.4$ and γ_{opt} = 1.6 that achieve $C_{P,opt}$= 0.76. Additionally, according to Eq. 3.8 increasing γ causes more increase to the power coefficient of the turbine.

3.1.1. Temperature profile of the collector

The solar Chimney Power Plant (SCPP) is influenced by many parameters that influence the performance of the turbine; however, the solar radiation and mass flow rate are essential variables, which should be studied. The collector is divided into sections at radial position and I applied Eqs. 3.28 and 3.26 on every section, I calculate variation of the temperature through the radial direction of the collector. Fig. 3.1 shows the variation of the temperature profile with solar radiation at constant mass flow rate of 796.96 Kg/s. The increase in the solar radiation causes more increase in the outlet temperature of the collector, but the temperature differences between the inlet and the outlet of the collector, ΔT_C, are 8.66, 15.17 and 19.80°C at solar radiation 650, 850, and 1050 W/m^2 respectively. Fig. 3.1 clearly shows that the temperature difference is reverse proportional to the solar radiation, because of the increase the heat loss into a surrounding with increasing temperature. For generating more power, the solar radiation also suffers from other limitation; it depends on the weather condition so this variable is not controllable.

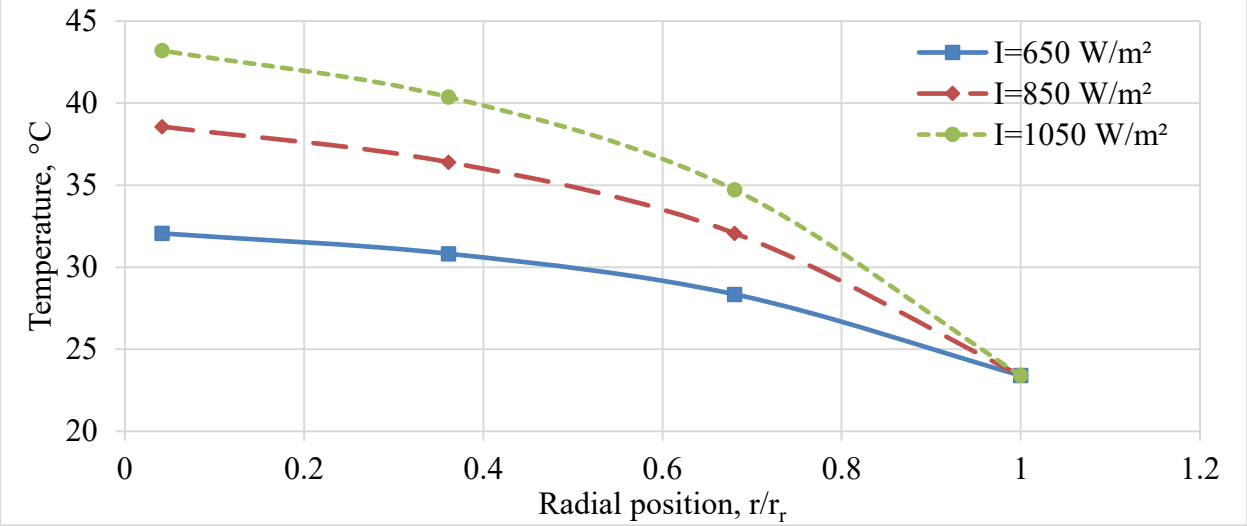

Fig. 3.1. Temperature profile inside the collector at different solar radiation

Fig. 3.2 shows the variation of the temperature profile at the different mass flow rate with the constant solar radiation of 850 W/m^2. The outlet temperature of the collector, T_2, is reverse proportional to the mass flow rate. On the other hands, the mass flow rate is directly proportional to the produced power. Thus, the optimization value of mass flow is investigated for generating more produced power.

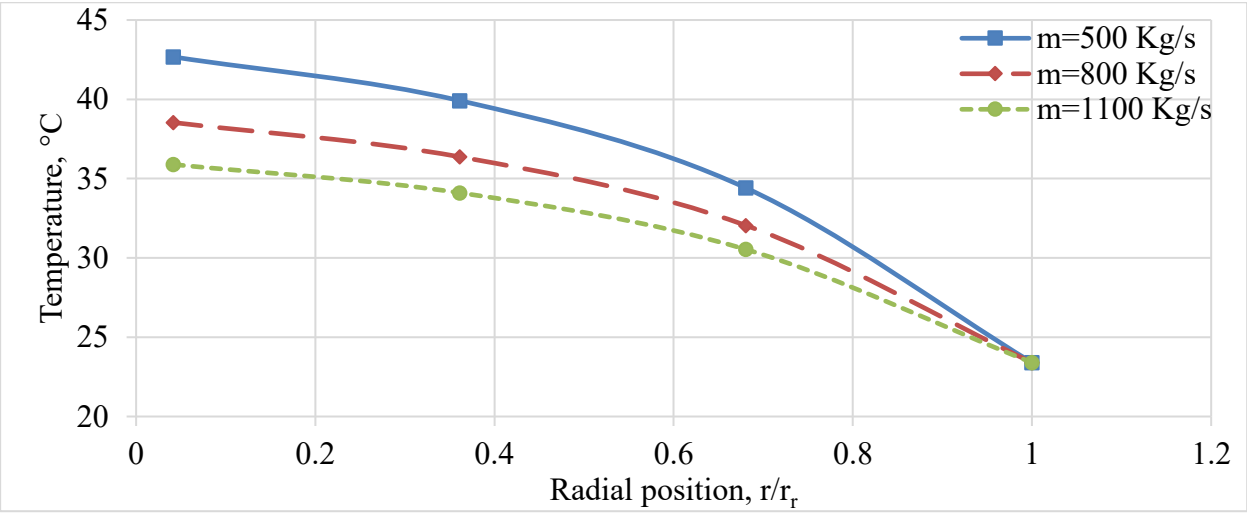

Fig. 3.2. Temperature profile inside the collector at different mass flow rate

3.1.2. The effect of mass flow rate

The influence of the mass flow and solar radiation on the output power is shown in Fig. 3.3. The behaviour of the curves is in good agreement with the result that was achieved by Koonsrisuk and Chitsomboon, (2013). The maximum power output is a function of the mass flow and solar radiation. So, the recommendation for optimum operation of the SCPP follows up the line of the maximum power, which is shown in Fig. 3.3. This can be applied by changing the turbine speed or changing the blade setting angle.

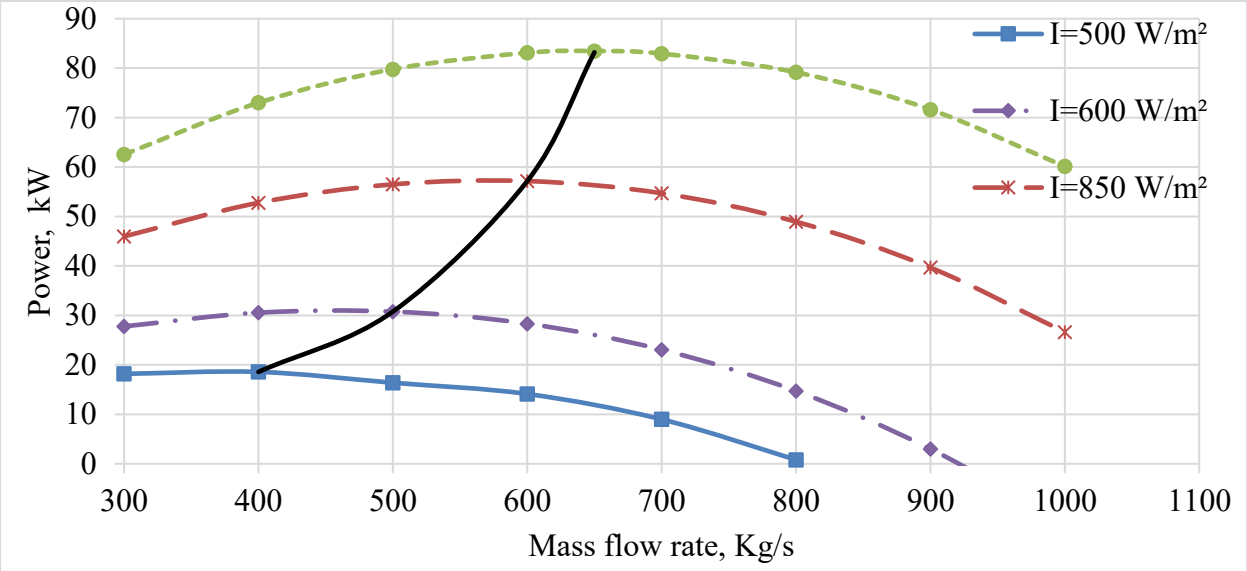

Fig. 3.3. Influence of the mass flow and solar radiation on the outlet power

The variation of the diffuser velocity speed-up ratio, γ, with mass flow and solar radiation is shown in Fig. 3.4. We can clearly notice that the range value of γ is insignificant variation from 1.6423 to 1.639 about 0.2012%. And the above-calculated value of γ is approximately equal to the average range, as shown in Fig. 3.4. As a consequence of this discussion, I will take γ equal 1.6403a new design.

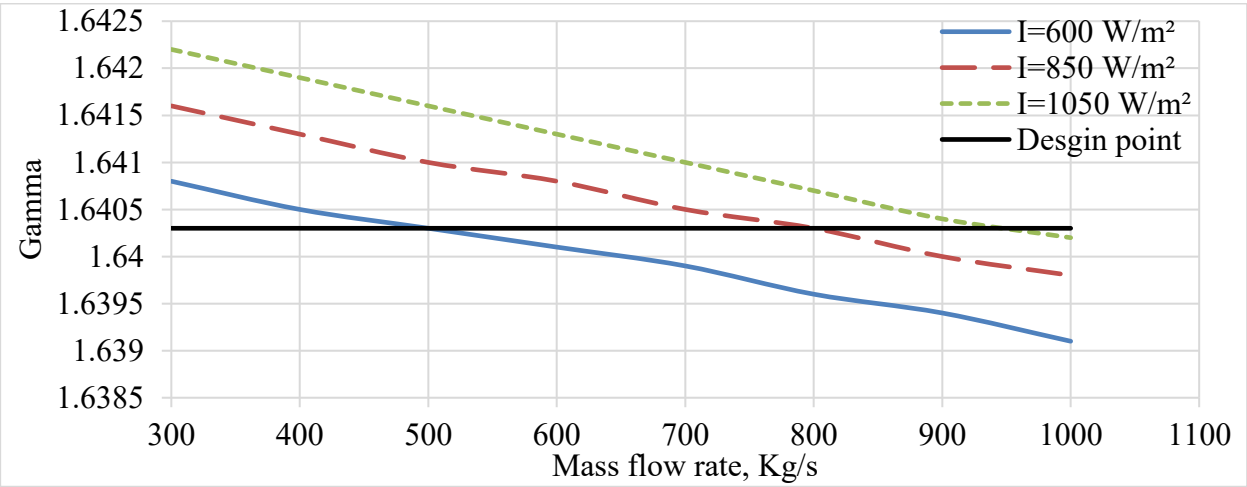

Fig. 3.4. Variation of the diffuser velocity speed-up ratio with mass flow and solar radiation

3.2. The methodology of turbine design working on SCPP

Based on the aerodynamic analysis and the optimization of a shrouded turbine blade, I implemented it within the MATLAB code to calculate the chord distribution and twist angle of the blade. This code also applies tip loss correction as from of Shen *et al.*, (2005). To validate the

code, the comparison of its result and result of Vaz and Wood, (2016) that I have done using the same input data that is shown in reference(Vaz and Wood, 2016), as shown in Fig. 3.5. Vas and Wood compared data from their optimization and National Aerospace Laboratory (NAL) design to show the improvements that were achieved by using their optimization.

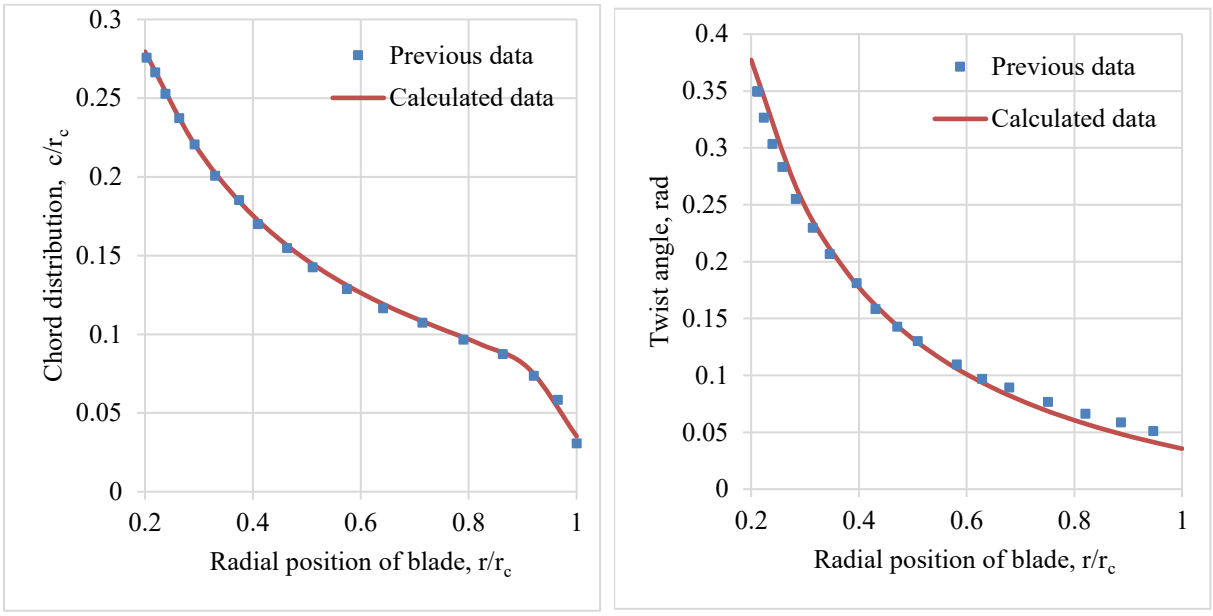

a- Chord distribution b- Twist angle

Fig. 3.5. Comparison of calculated data and data of (Vaz and Wood, 2016)

Finally, the chord distribution and twist angle of optimization blade shape of SCPP is shown in Fig. 3.6 using the design parameter in Table 3.3.The main aim of the new design is achieving more power than the previous turbine. An integration of Eq. 2.4 using the trapezoidal method calculate the power coefficient of the new design is 0.45, and then calculate the theoretical output power is 55.752 kW. The increase in the output power is 15.19% compared to the original design. I have been created the 3D of the design blade using SOLIDWORK that shown in Fig. 3.7.

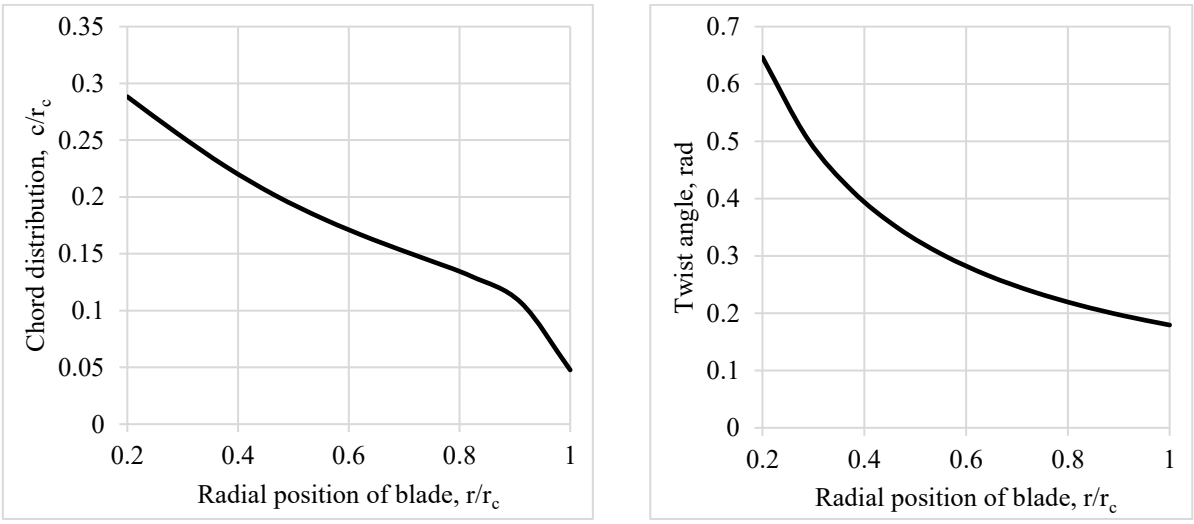

a- Chord distribution b- Twist angle

Fig. 3.6. The Designed blade shapes

Table 3.3. design parameter using by optimization code

Turbine radius, *Rt*	5 m
Hud radius , R_h	1 m
Number of blades , *B*	4
Blade airfoil	FX W-151-A
Turbine speed ,Ω	100 rpm

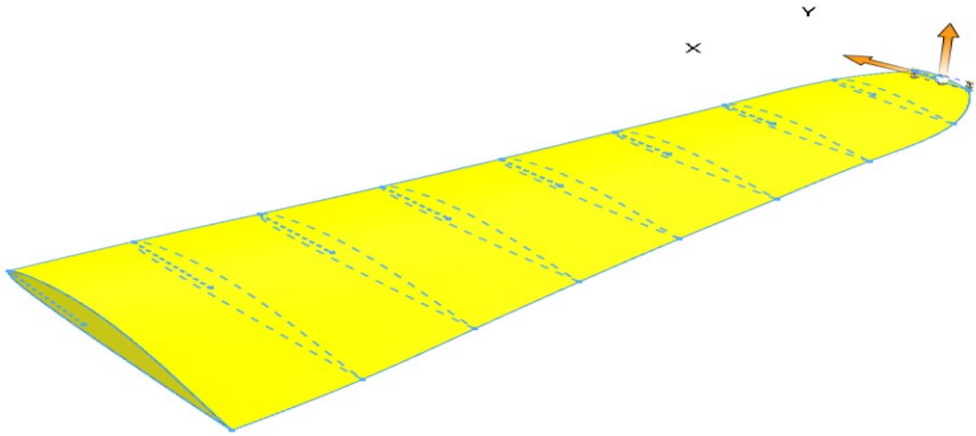

Fig. 3.7. 3D of designed blade for SCPP

3.3.The influence of the solar collector shape

The solar chimney power plant system is proposed to produce electric power on a large-scale, utilizes solar heating and chimney effect for increasing kinetic energy of the ambient air that drives wind turbines to produce electric power. High insolation and over 90 % available desert lands are two main conditions that motivated the development of thermal solar power plants as generally, and solar chimney power plant especially for electrical energy productions (Mostafa, Sedrak and Dayem, 2011). Thus, thermal solar electricity project is a perfect solution to utilize the Aswan weather condition, that motivated Science and Technology Development Fund (STDF) of Egypt and Federal Ministry of Education and Research (BMBF) of Germany funded prototype of SCPP in Aswan, Egypt as a joint project. The experimental work is carried out on the Aswan prototype that is A small-scale solar chimney type. Table 3.4 shows the dimension of this prototype.

Table 3.4. Dimension of Aswan solar chimney prototype

Location	Dimension	Description
Diameter of chimney	1m	Steel tube of 0.8 mm thickness
Height of chimney	20 m	
Solar collector	28.5 m side length	Square shape collector
The height of inlet collector	1.25m	
The height of outlet collector	1.5m	

The collector has two common shapes: circular collector and square shaped collector, for studying the more efficient shape, we made the CFD model for both shapes. Table 3.5 shows the calculated results of both shapes of the collector. The geometric calculation shows the square shape collector increases the inlet area by 11.4 % than the circular collector. The airflow isn't a uniform distribution on the inlet area because of low inlet air velocity, the reverse airflow takes a place on the geometric inlet area and the effective inlet area present the actual part of a geometric inlet area

that allows the airflow inside the collector. The square collector increases the effective inlet area by approximately 30% at the same inlet height, the mass flow rate of square shape is consequently increased by 4.3 %. However, solar radiation exposed to the same surface area in both cases, but the circular shape achieves 0.683 °C higher than the square shape collector of the average exit temperature. Due to the increase in the mass flow rate, the output power that produces increases by 7.6 % based on the square calculation results.

Table 3.5. CFD results of circular and square collectors

	Circular collector	Square collector	Percentage
Geometric inlet area, m^2	151.55	171	11.4%
Effective inlet area, m^2	101.026	144.3	30%
Mass flow rate, Kg/s	13.4487	14.0507	4.3%
Outlet temperature of collector ,^{0}C	45.124	44.441	-1.5%
Output power, W	329.237	356.151	7.6%

3.3.1. The square shape collector

Using a velocity vector tool in ANSYS CFX-Post, we can get more analysis of the air velocity inside the collector. Fig. 3.8 shows the velocity vector field at height 0.65 m from the ground (approximately mid-span) and radial direction of the velocity vector field of the square collector. Fig. 3.8-a shows the shortest radial direction from the mid-span of the square side to the centre of the collector and Fig. 3.8-b shows the longest radial direction from the corner of the square side to the centre of the collector. The differences between Fig. 3.8-a and Fig. 3.8-b results from the different length of the airflow path.

The velocity distribution has a considerable effect in creating temperature distribution inside the collector. Fig. 3.9 shows the temperature contour at approximately mid-span from the ground (the same plane of the velocity vector) and the radial direction of the temperature contour of the square collector.

3.3.2. The circular shape collector

For demonstrating the difference of the performance between the circular shape and square shape collectors, we follow the similar pattern of the calculated result for the circular shape collector. Fig. 3.10 shows the velocity vector field at height 0.65 m from the ground (approximately mid-span) and radial direction of the velocity vector field of the circular collector. The airflow suffers from a high turbulence and some reverse flow at the inlet as shown in Fig. 3.10-b and Fig. 3.10-a, both of these paths have the same length. However, the longest paths from corners to the centre of the collector has more smooth airflow at the inlet area, as shown in Fig. 3.8-a. Consequently, the square shape collector achieved a larger mass flow rate of air.

Fig. 3.11 shows the radial direction of the temperature contour of the circular collector and the temperature contour at approximately mid-span from the ground (the same plane of the velocity vector). The temperature distribution inside the circular shape collector is exceedingly regularly, as shown in Fig. 3.11-a. The turbulent flow assists to increase the heat transfer by an increasing the length of flow streamline and mixing processes of a laminate of the fluid. However, the square shape collector has a more turbulent flow pattern, as shown in Fig. 3.9, it achieves less the average

exit temperature of the collector by -1.6 % than the circular collector, because of the higher mass flow rate.

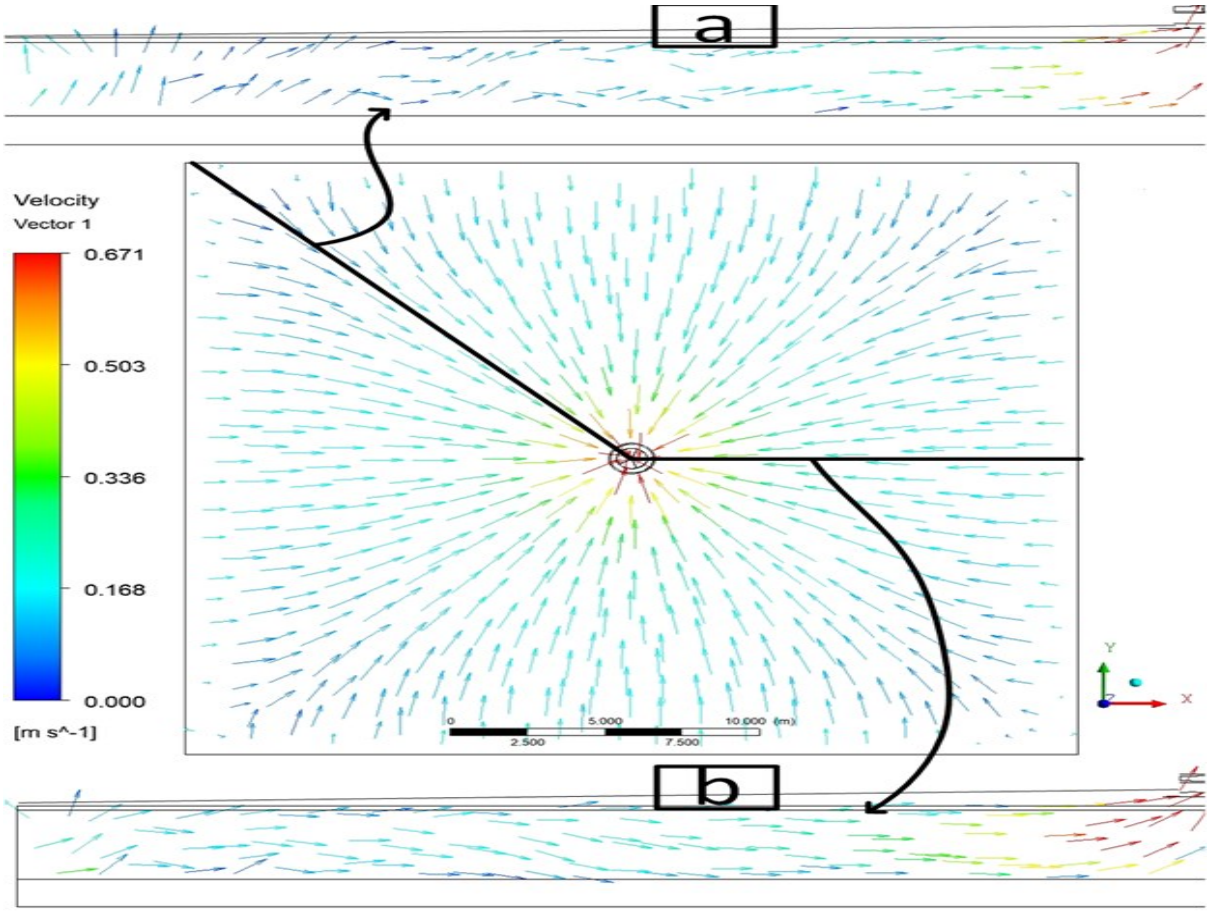

Fig. 3.8. Velocity vector inside the square shape collector

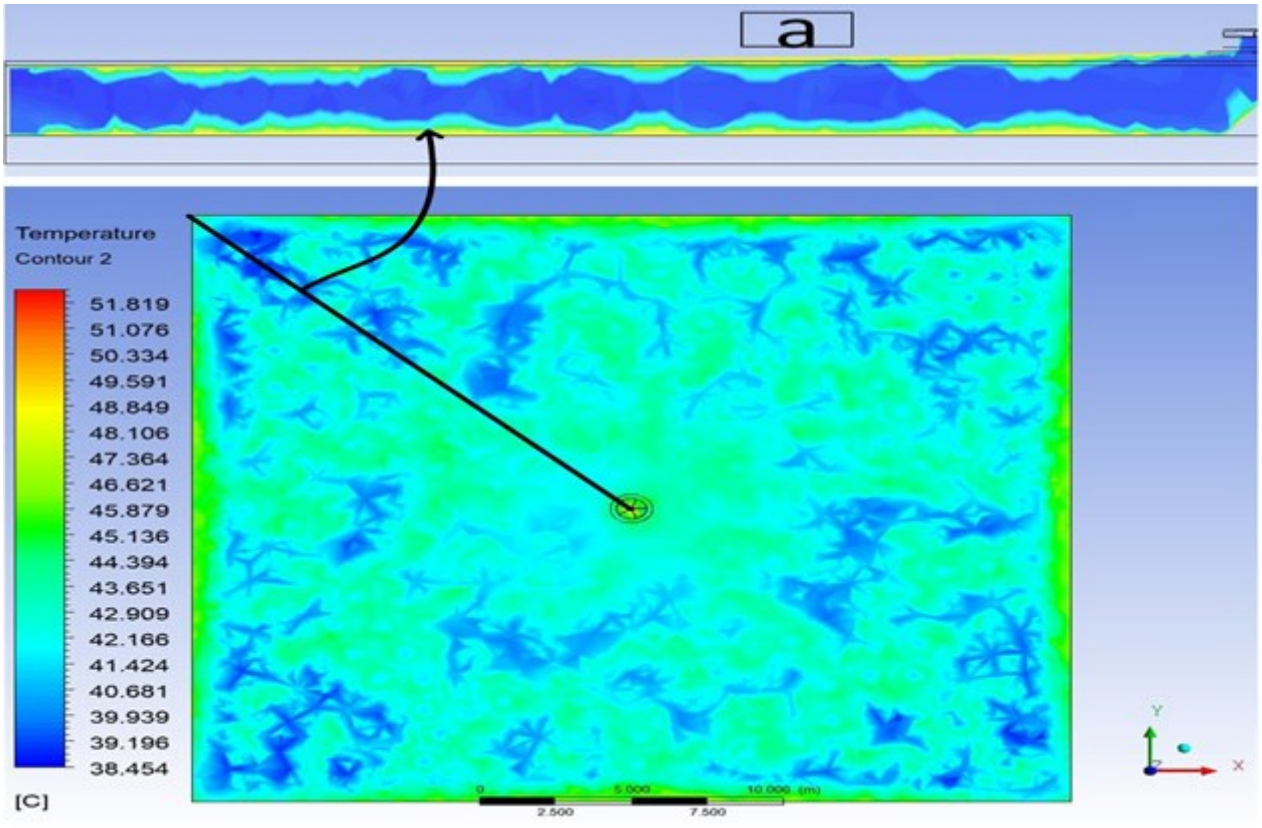

Fig. 3.9. Temperature distribution of the square collector

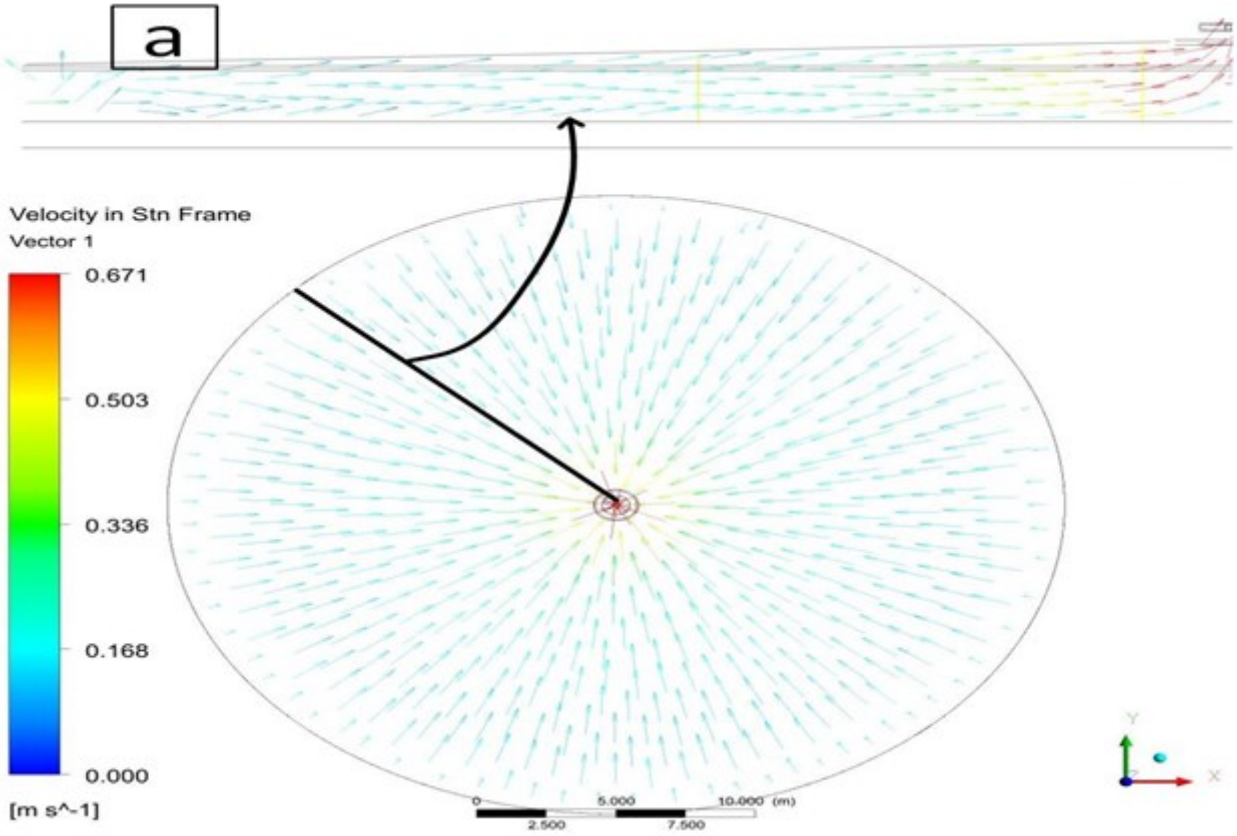

Fig. 3.10. Velocity vector of the circular shape collector

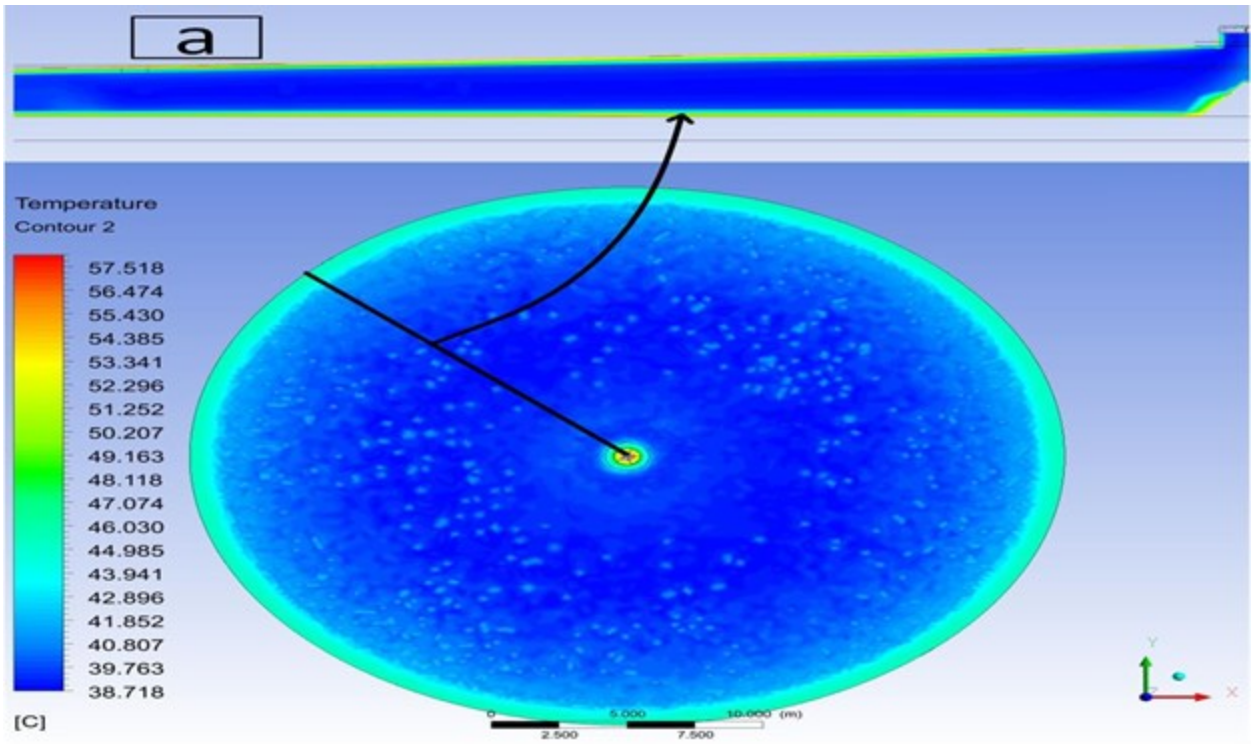

Fig. 3.11. Temperature distribution of the circular shape collector

4. NEW SCIENTIFIC RESULTS

In this section the unique scientific results investigated in my study are shown as following:

1. *Development of a modified mathematical model of solar chimney power plant*

My modified mathematical model calculates the temperature distribution of collector and flow field inside the SCPP with fewer assumptions than the existing models in the literature in the theoretical analysis. The aim of this model is to calculate the essentials terms of the turbine design. SCPP is influenced by many parameters that effect of the performance of the turbine, however, the solar radiation and mass flow rate are essential variables, which should be studied. The collector is divided to sections at radial position and I applied my MATLAB code on at every section, my model calculates variation of temperature through the radial direction of the collector

To validate the mathematical model, calculated results were compared with the experimental results of the prototype from Manzanares, Spain. The deviation of collector loss coefficient, collector exit temperature, pressure drop of turbine, and output power are 1.808%, 5.943%, 6.668% and 0.5909% respectively, which are acceptable values.

My new mathematical model shows that the output power of SCPP is a function of the mass flow and solar radiation. So, the recommendation for optimum operation of the SCPP using an optimization algorithm, which can be applied by changing the turbine speed or changing the blade setting angle.

2. *New methodology of turbine design working on SCPP*

I presented a new design of axial flow turbine based on the blade element theory (BET), which is modified to improve the performance of the wind turbine by the concept of argument diffuse wind turbine (ADWT). The speed ratio, γ, and tip speed ratio, λ, are the main parameters that control of the blade shape and make the blade more suitable for its enclosure.

Aerodynamic analysis of the wind turbine consists of actuator disc theory that applies the momentum concept on the infinite number of the blade rotor, rotor disc theory that takes into account the rotation effect of the rotor, and blade element theory (BET) that considered the force acting on an element of the blade. The analysis is incorporated with the diffuser duct effect to make the blade more sensitive and to have efficient performance during its working inside the duct. By solving equations of the BET theory, the chord distribution and twist angle are obtained presenting the final shape of the blade turbine.

Blade shape of solar chimney turbine is optimized to achieve maximum output power possible form SCPP. My optimization procedure is implemented using iteration algorithm within MATLAB. The interface between MATLAB and XFOIL is used to obtain FX W-151-A aerofoil data. MATLAB code is validated with the previous design that presented by Vaz and Wood,(2016). Power coefficient of the presented design has reasonably value reaching 0.45 at design point condition (5.5 of tip speed ratio), which is higher than Betz limit that used for free wind turbine. Therefore, the output power is improved by 15.19 % to reach 55.752 KW while the original design achieves 48.4 KW at design point.

3. *The influence of the solar collector shape*

I used CFD to study velocity and temperature distribution inside collectors that have the square and circular shapes with same surface area. The 3D CFD model of the whole SCPP with turbine

and radiation model is carried out. To achieve that purpose, I used ANSYS CFX software for solving the governing equation with the k-omega turbulence model and validate calculated results by comparing to experimental data of Aswan prototype. The instantaneous temperature distribution at different sections and rotational speed of the turbine generator unit are measured during a period of time. Then, I compared the two shapes of the solar chimney collector at constant surface area.

The collector has two common shapes: circular collector and square shaped collector with same area, for studying the more efficient shape, the geometric calculation shows the square shape collector increases the inlet area by 11.4 % than the circular collector. The airflow isn't a uniform distribution on the inlet area because of low inlet air velocity, the reverse airflow takes a place on the geometric inlet area and the effective inlet area present the actual part of a geometric inlet area that allows the airflow inside the collector. The square collector increases the effective inlet area by approximately 30% at the same inlet height, the mass flow rate of square shape is consequently increased by 4.3 %. However, solar radiation exposed to the same surface area in both cases, but the circular shape achieves 0.683 ºC higher than the square shape collector of the average exit temperature. Due to the increase in the mass flow rate, the output power that produces increases by 7.6 % based on the square calculation result at constant surface area.

5. CONCLUSIONS AND SUGGESTIONS

Solar chimney power plant (SCPP) is a new technology that uses solar air heating and chimney effect to produce electricity. The operating conditions of SCPP impose special properties on the solar chimney turbine. So, the turbine has characteristics mixing between gas turbine and wind turbine. The main aim of this study is to determine the more suitable design theory for a turbine that works inside SCPP. Subsequently, we use CFD simulation to compare performances of three different designs: DAWT (diffuser argument wind turbine) design, MTFM (Matrix through-flow method) design, and Aswan design that is applied classic blade element theory.

The CFD results present the distribution of velocity and temperature for studying the square and circular shape of collectors. The conclusion that the square collector achieved higher output power than the circular collector by 7.6 % at the same surface area Exposed to solar radiation, additionally, the square shape causes a turbulent flow pattern due to change in flow stream lengths that assists to improve the heat transfer process.

The mathematical model is presented, it depends on easily measurable quantities to estimate the performance of SCPP and calculate the design parameter of a solar chimney turbine. The validation of the mathematical model is carried out by comparing its result with the experimental data from the prototype in Manzanares. The comparison shows good agreement.

The blade shape of the solar chimney turbine is optimized to achieve maximum output power possible from SCPP. The optimization procedure is implemented using an iteration algorithm within MATLAB. The interface between MATLAB and XFOIL is used to obtain FX W-151-A aerofoil data. MATLAB code is validated with the previous design that is presented by Vaz and Wood, (2016). Power coefficient of the presented design has reasonable value reaching 0.7250 at design point condition, which is higher than the Betz limit. Additionally, the output power is improved by 15.19 % to reach 55.752 kW while the original design achieves 48.4 kW.

The blade that was designed for SCPP, is manufactured by 3D printing, then the whole rotor of the turbine and indusial turbine are tested within the wind tunnel. The pressure drop of the designed turbine is higher than the industrial turbine by 1.5 times approximately. Generally, the designed turbine has more performance than the industrial one. The highest power coefficient of the designed turbine is 0.45, while the highest power coefficient of the industrial turbine is 0.31. the designed turbine produces 12.55% higher than the industrial one as average increase on all points.

For the future works; The modern energy field recently depends on the renewable energy system such as a solar chimney power plant (SCPP). The field testing of SCPP is a main aim. The solar radiation is source of energy in SCPP, which depend on climate condition of operation location. The field measurement provides realistic data that forms the real performance of the solar chimney system, so, the field experiment is an essential step should be carried out before proposing the SCPP in the markets. Studying the heat storage system takes also a great part of the development of the SCPP system.

For same reasons that mentioned above (making commercial system and increasing both reliability and expansibility), studying the ability of cooperation between Solar chimney system with other solar systems such as photovoltaic or Water desalination will be focused. Hybrid system increases utility of solar energy, it improves effectiveness of the solar system and expands the solar appliances.

6. SUMMARY

AXIAL FLOW TURBINE FOR SOLAR UPDRAFT TOWERS

In this work, a chief aim is an improvement of performing solar chimney power plants (SCPPs) by making its turbine more efficient, The SCPP is a modernistic solar technology that powered combination of solar heating and chimeny effect. We developed a comprehensive mathematical model to understand the working environment of the turbine and to calculate the parameters of design, this model calculated the pressure and temperature at some position of SCPP and mass flow rate through it by the iterative code that is implemented by MATLAB.

Blade element theory with a diffuser is selected for designing the solar chimney turbine, the theory takes into account the shape of surrounding duct, that give the designed blades more sensitivity and harmony with its duct. the parameters of the blade geometry (chord distribution and twist angle) calculated by MATLAB code, which optimize the blade element-momentum theories equations to achieving maximum output power. The MATLAB code is interfaced with *XFoil* program to load the results data of the aerofoil which you can then use in iterative algorithm.

To calculate the design parameter, the comprehensive mathematical model is carried, which has an ability to describe the flow inside solar chimneys. An iteration algorithm is implemented using MATLAB to obtain optimization of the turbine blade chord and twist angle distributions in the presence of a diffuser. The comparison of the mathematical model results and experimental data of Manzanares prototype reveal the good agreement, validating our mathematical model.

Computational fluid dynamics technique (CFD) is used also for studying the performed of SCPP and comparing three different designs of the solar chimney turbine for a substantiation the more suitable theory to design solar chimney turbines. We solved the governing equation of the whole SCPP unit using the computational fluid dynamics module of ANSYS CFX v18.1. The computational results were compared with experimental data to validate it. The testing of SCPP prototype has been carried out in Aswan, Egypt, where the climate is suitable for commercial SCPP units. The theoretical comparison between the three different designs showed that the highest output power is achieved by the design that applied DAWT (diffuser argument wind turbine) theory. Three dimensional CFD simulations were made to calculate the temperature and velocity distribution inside two different shapes of SCPP collector. The conclusion is that the square-shaped collector achieved higher output power than the circular collector by 7.6 % at the same surface area exposed to solar radiation.

The blade that was designed for SCPP, is manufactured by 3D printing. we measured the power, flow rate, rotational speed and pressure drop of the designed and industrial turbines within the wind tunnel, and the power coefficient of the turbines are calculated by measured values. The pressure drop of the designed turbine is higher than the industrial turbine by 1.5 times approximately. Generally, the designed turbine has more performance than the industrial one. The highest power coefficient of the designed turbine is 0.45, while the highest power coefficient of the industrial turbine is 0.31. The designed turbine produces 12.55% higher than the industrial one.

7. MOST IMPORTANT PUBLICATIONS RELATED TO THE THESIS

Refereed papers in foreign languages:

1. **A-Elmagid, W. M.** and Keppler, I. (2017) 'Axial flow turbine for solar chimney', *Hungarian Agricultural Engineering*, (32), pp. 29–37. doi: 10.17676/hae.2017.32.29.
2. **A-Elmagid, W. M.**, Keppler, I. and Molnar, I. (2020) 'Efficient Axial Flow Turbine for Solar Chimney', *Journal of Thermal Science and Engineering Applications*. ASME International, 12(3). doi: 10.1115/1.4044903.
3. **A-Elmagid, W. M.** et al. (2020) 'Studying the collector performance of updraft solar chimney power plant', *Journal of Engineering and Technology (JET)*, Vol. 11, No. 1, pp. 1-8, ISSN: 2180-3811
4. **A-Elmagid, W. M.** et al. (2021) 'A Numerical comparative study of axial flow turbines for solar chimney power plant', *Case Studies in Thermal Engineering*, 26, p. 101046. doi: 10.1016/j.csite.2021.101046.
5. **Walid M.A Elmagid**, 'Testing axial flow solar chimney turbine using wind tunnel' (in progress)

International conference proceedings:

6. **A-Elmagid, W. M.**, and Keppler I. (October 16-19- 2017). Axial Flow Turbine for Solar Chimney. Synergy International Conferences - Engineering, Agriculture and Green Industry Innovation. Gödöllő, Hungary.

International conference abstracts:

7. **A-Elmagid, W. M.** et al. (2019). Load analysis for blades of a solar chimney turbine using Fluid–structure interaction modelling. Synergy International Conferences - Engineering, Agriculture and Green Industry Innovation, Gödöllő, Hungary, November 4-6, 2019. Szent István University Faculty of Mechanical Engineering, (2019) pp. 20, ISBN: 978-963-269-854-0.
8. **A-Elmagid, W. M.** "Design and testing of a small turbine blade at low speed wind", 22th Workshop on Energy and Environment (EE 2016), December 1-2, 2016, Gödöllő, Hungary
9. **A-Elmagid, W. M.** "Theoretical Investigation of Solar Chimney Power Plant Installed in Aswan City", 6th Scientific Workshop by Egypt's Office for Cultural and Educational Relations Vienna, 27th of April 2017
10. **A-Elmagid, W. M.** "Mathematical model of the solar updraft chimney", 23rd Workshop on Energy and Environment (EE 2017), November 30 - December 1, 2017, Gödöllő, Hungary